Supporting Information

Bengtson et al. 10.1073/pnas.0812460106

SI Text

Sample Handling. In view of the grave doubts that have been cast on the indigenous nature of the "shelly" fossils reported from the Lower Vindhyan rocks (see main text), special care was taken to avoid contamination in the field and in the laboratory. Each sampling spot was documented with geographic coordinates and photographs (Fig. S1). The samples were split into 2 parts: 1 that was sent to the Wadia Institute of Himalayan Geology in Dehra Dun, and 1 that was shipped directly from the field to the Swedish Museum of Natural History in Stockholm. Only the "Swedish" samples were used in the present study.

The coordinates for the sampling spots are given in latitudinal–longitudinal degrees and decimal minutes, as obtained from a hand-held global positioning system unit under clear view of the sky. The lateral precision is likely to be within ±5 m.

Samples for microfossil extraction were cleaned in a bath of 1% NaClO for 2 h, followed by mechanical brushing of loose material. They were thereafter dissolved in 10% acetic acid, buffered to approximately pH 5. The residues were wet-sieved through a set of new stainless-steel sieves that had not previously been used for other purposes. They were thereafter manually examined and sorted under a binocular microscope.

SHRIMP U–Pb Zircon Data for Samples from the Porcellanite Formation. Two samples of light-brown mudrock (Ind06111202 and Ind 06111203; see sample information in Fig. S1) from the Porcellanite Formation (Semri Group, Lower Vindhyan) were used to extract zircons for U–Pb dating. Polished thin sections of the samples show that the rocks are tuffaceous containing mostly cuspate and platy glass shards (Fig. S2), as well as less-common pumice shard fragments, within a matrix of fine-grained ash. The shards have been replaced by chert. Minor constituents include angular silt-sized fragments of quartz and K-feldspar, as well as rare equant zircon crystals. The abundance of former glass shards along with quartz, K-feldspar, and minute euhedral zircon crystals indicates that the tuffaceous mudrocks were the products of explosive felsic volcanism.

Both samples of tuffaceous mudrock were crushed, and heavy minerals were separated using heavy liquids. The concentrate was passed through a Franz magnetic separator, and the nonmagnetic fraction was again processed with heavy liquids to obtain a final zircon separate. Abundant zircon crystals were obtained from both samples. Most crystals are euhedral and range in shape from equant to prismatic (Fig. S3).

Approximately 200 zircon crystals were hand picked from each separate and mounted along with the 2 main reference standards, BR266 and CZ3, in a 25-mm-diameter epoxy disc (Mount 07–34). Data were collected under standard SHRIMP operating conditions for zircon (ref. 1 and references therein), using BR266 as the Pb/U reference standard and CZ3 for U and Th abundance determination. Data reduction was carried out using Squid 1 software (2).

Ind 06111202 (Mount 07–34A). Data for sample 07–34A (Fig. S4 and Table S1) are almost all concordant, and the $^{208}Pb/^{232}Th$ of the concordant data are self-consistent, so there is no evidence in these data for any substantial isotopic disturbance in the zircon crystals. Two analyses with >0.5% common Pb and a single discordant analysis have been omitted from age considerations. The remaining 27 analyses have a weighted mean $^{207}Pb/^{206}Pb$ age of 1,630 ± 8 Ma, with a mean square of weighted deviates (MSWD) of 1.9. The excess scatter is largely attributable to analysis A.4–1, which is a fairly strong outlier and a likely xenocryst. Omitting this analysis leaves 26 analyses with a weighted mean $^{207}Pb/^{206}Pb$ age of 1,629 ± 7 Ma (MSWD = 1.6). A probability plot of $^{207}Pb/^{206}Pb$ dates from the 26 retained analyses suggests a possible bimodal distribution. However, this is too weak to be considered definitive, and mixture modeling (3) as a 2-component distribution gives a "relative misfit" of 0.96 (i.e., little better than the single-population distribution). Thus, the weighted mean age of 1,629 ± 7 Ma is interpreted as the likely age of the main zircon population.

Ind 06111203 (Mount 07–34B). The zircon crystals analyzed from sample 07–34B have distinctly higher U contents than those in 07–34A. The data for 07–34B (Fig. S5 and Table S2) are more scattered than for 07–34A, reflecting considerably more open-system behavior in these crystals, consistent with radiation damage from the high-U contents. Almost half of the analyses (Table S2) are discordant (>±5%) or have high common Pb contents (>0.5%) and are subsequently unsuitable for age determination. One other high-U analysis that is an extreme young outlier in $^{207}Pb/^{206}Pb$ (B.9–1), and which is only marginally concordant, has also been omitted from consideration. Among the remaining 18 analyses (Fig. S5), B.2–1 is very imprecise owing to primary ion beam instability, but this has no bearing on the weighted mean $^{207}Pb/^{206}Pb$ age of 1,626 ± 7 Ma (MSWD = 1.3).

Summary. The SHRIMP U–Pb dates obtained from the 2 tuffaceous mudrocks (1,629 ± 7 Ma and 1,626 ± 7 Ma) are interpreted as the time of zircon crystallization from a magma coeval with eruption and therefore to provide close estimates for the age of deposition. The dates are stratigraphically consistent with each other and previous radiometric dates and show that the Porcellanite Formation was deposited at approximately 1,628 Ma, consistent with a late Palaeoproterozoic and early Mesoproterozoic age for the lower Vindhyan.

Pb Isotope Analysis of Jankikund Phosphorites. Pb isotope data (Table S3) from 2 phosphorite samples from Jankikund were obtained for this study using finely ground rock powder prepared in an agate pestle and mortar. Sample Ind06110701 was subject to a single whole-rock dissolution; 2 separate whole-rock dissolutions were made of sample Ind06110805. Whole-rock dissolution was performed using cold 6 M HCl for 2 h followed by a concentrated hydrofluoric acid (HF) treatment of the dried-down residue. For an additional subsample of Ind06110805, the HCl leachate solution was decanted off and treated as a separate sample from the HF-soluble residue.

Pb was extracted from the 3 whole-rock samples, the leachate, and the residue using conventional anion-exchange chromatography using HBr. Isotope analysis was performed using a Micromass (GVI) Isoprobe inductively coupled plasma multicollector mass spectrometer equipped with a Cetac MCN6000 desolvating nebulizer. Pb samples from the ion-exchange procedure were dissolved in 1 M HCl and mixed with a Tl tracer to facilitate mass bias correction. Analyses of unknown samples were interspersed in an automated sequence with NBS981 and NBS982 standard Pb solutions, as well as an in-house monitor solution of known isotopic composition. Pb isotope ratios of unknowns were corrected for instrumental mass fractionation using the $^{203}Tl/^{205}Tl$ ratio, and a further minor correction was applied to correct the average NBS981 value from the session to

the accepted values (5). External precision for the individual analytic session was 0.025% [2 relative standard deviations (RSD)] on $^{207}Pb/^{204}Pb$ and 0.028% (2RSD) on $^{208}Pb/^{204}Pb$. Data were regressed using the routines of Isoplot-Ex (6) assuming the U decay constant recommendations of Steiger and Jäger (7).

1. Smith JB, et al. (1998) The Sholl Shear Zone, West Pilbara: Evidence for a domain boundary structure from integrated tectonostratigraphic analyses, SHRIMP U-Pb dating and isotopic and geochemical data of granitoids. *Precambrian Res* 88:143–171.
2. Ludwig KR (2001) *SQUID 1.00: A User's Manual (Special Publication 2)* (Berkeley Geochronology Center, Berkeley, CA).
3. Sambridge MS, Compston W (1994) Mixture modelling of multi-component data sets with application to ion-probe zircon ages. *Earth Planet Sci Lett* 128:373–390.
4. Stacey JS, Kramers JD (1975) Approximation of terrestrial lead isotope evolution by a two-stage model. *Earth Planet Sci Lett* 26:207–221.
5. Todt W, Cliff RA, Hanser A, Hofmann AW (1996) Evaluation of a $^{202}Pb–^{205}Pb$ double spike for high precision lead isotope analysis. *Earth Processes: Reading the Isotopic Code (Geophysical Monograph 95)*, eds Basu A, Hart SR (American Geophysical Union, Washington, DC), pp 429–437.
6. Ludwig KR (1999) *Using Isoplot/Ex, Version 2.01: A Geochronological Toolkit for Microsoft Excel (Special Publication 1a)* (Berkeley Geochronology Center, Berkeley, CA).
7. Steiger RH, Jäger E (1977) Subcommission on Geochronology: Convention on the use of decay constants in geo- and cosmochronology. *Earth Planet Sci Lett* 36:359–362.

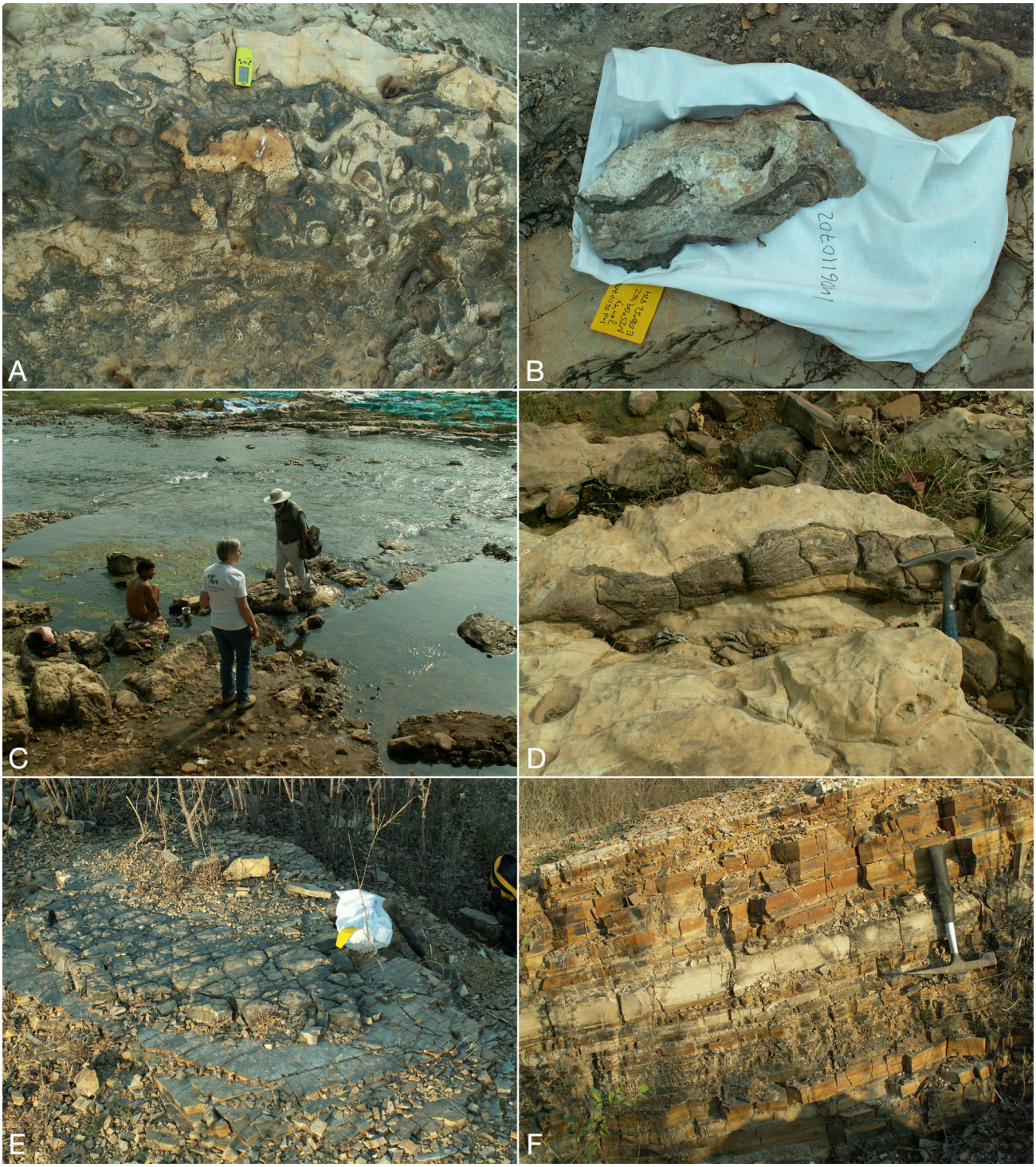

Fig. S1. Field photographs documenting sampling spots. (*A*) Sample Ind06110701. Tirohan Formation, Semri Group. Stromatolitic dolomitic limestone, with black phosphorite, Jankikund section, Chitrakoot. N25°09.462′ E080°51.814′. (*B*) Sample Ind06110702. Tirohan Formation, Semri Group. Stromatolitic dolomitic limestone, partly silicified, with black phosphorite, Jankikund section, Chitrakoot. N25°09.462′ E080°51.814′. (*C*) Locality of sample Ind06110804. Tirohan Formation, Semri Group. Stromatolitic columns with phosphatic clasts in between, Jankikund section, southwest corner of temple, Chitrakoot. N25°09.761′ E080°52.081′. (*D*) Sample Ind06110805. Tirohan Formation, Semri Group. Composite sample from different pockets of pebbly phosphorite, Jankikund section, 100 m south of temple, Chitrakoot. N25°09.808′ E080°52.189′. (*E*) Sample Ind06111202. Porcellanite Formation, Semri Group. Tuffaceous mudrock bed (beneath sample bag), weathered black; whitish in fresh fracture. Chopan railway exposure. N24°28.881′ E083°01.976′. (*F*) Sample Ind06111203. Porcellanite Formation, Semri Group. Tuffaceous mudrock bed (level at middle of hammer), weathered white; whitish in fresh fracture. Approximately 3 m below Ind06111202. Chopan railway exposure. N24°28.872′ E083°01.978′.

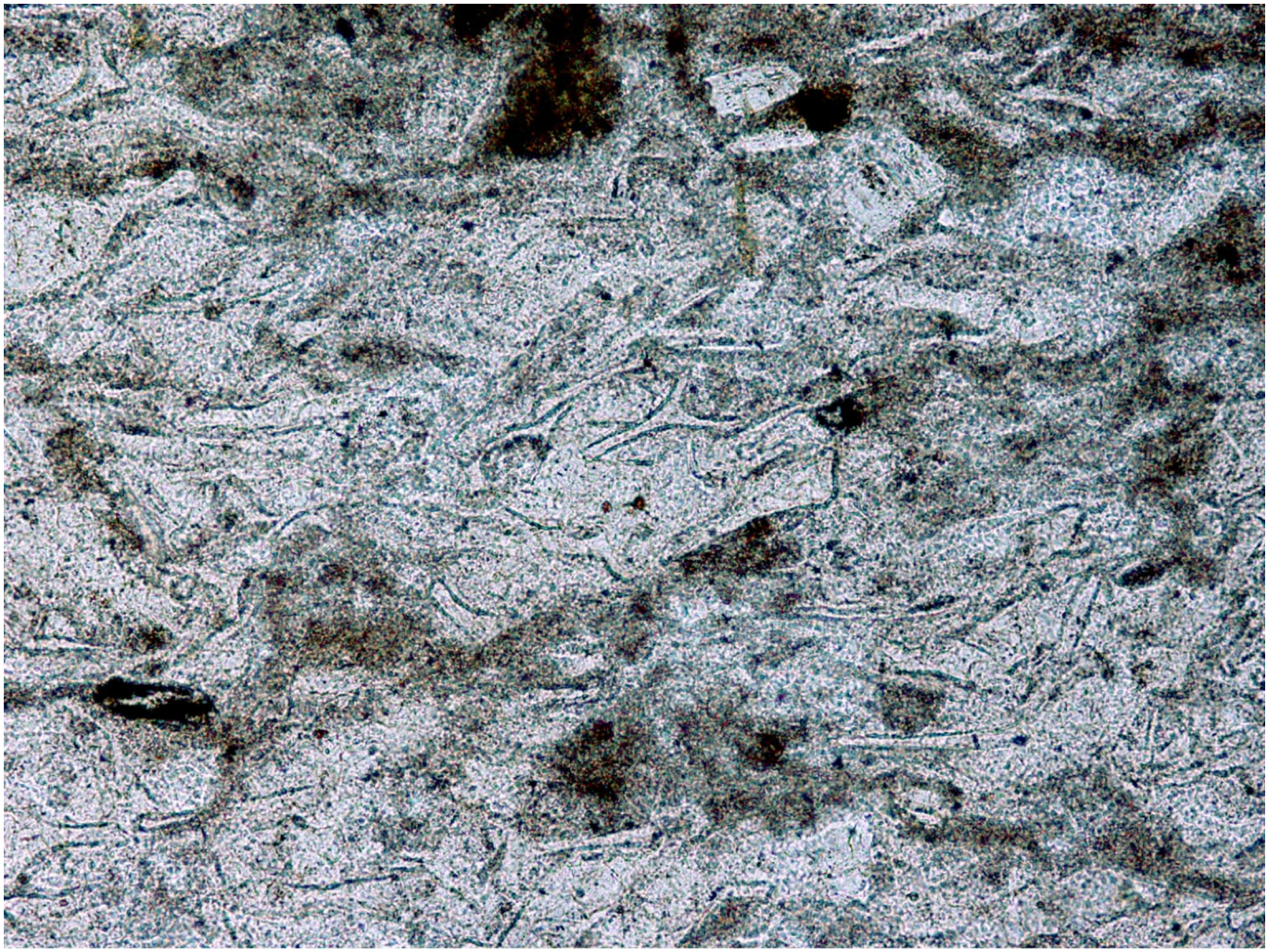

Fig. S2. Photomicrograph showing typical platy and cuspate glass shards in a fine-grained ash matrix. Plane polarized light. Sample Ind 06111203.

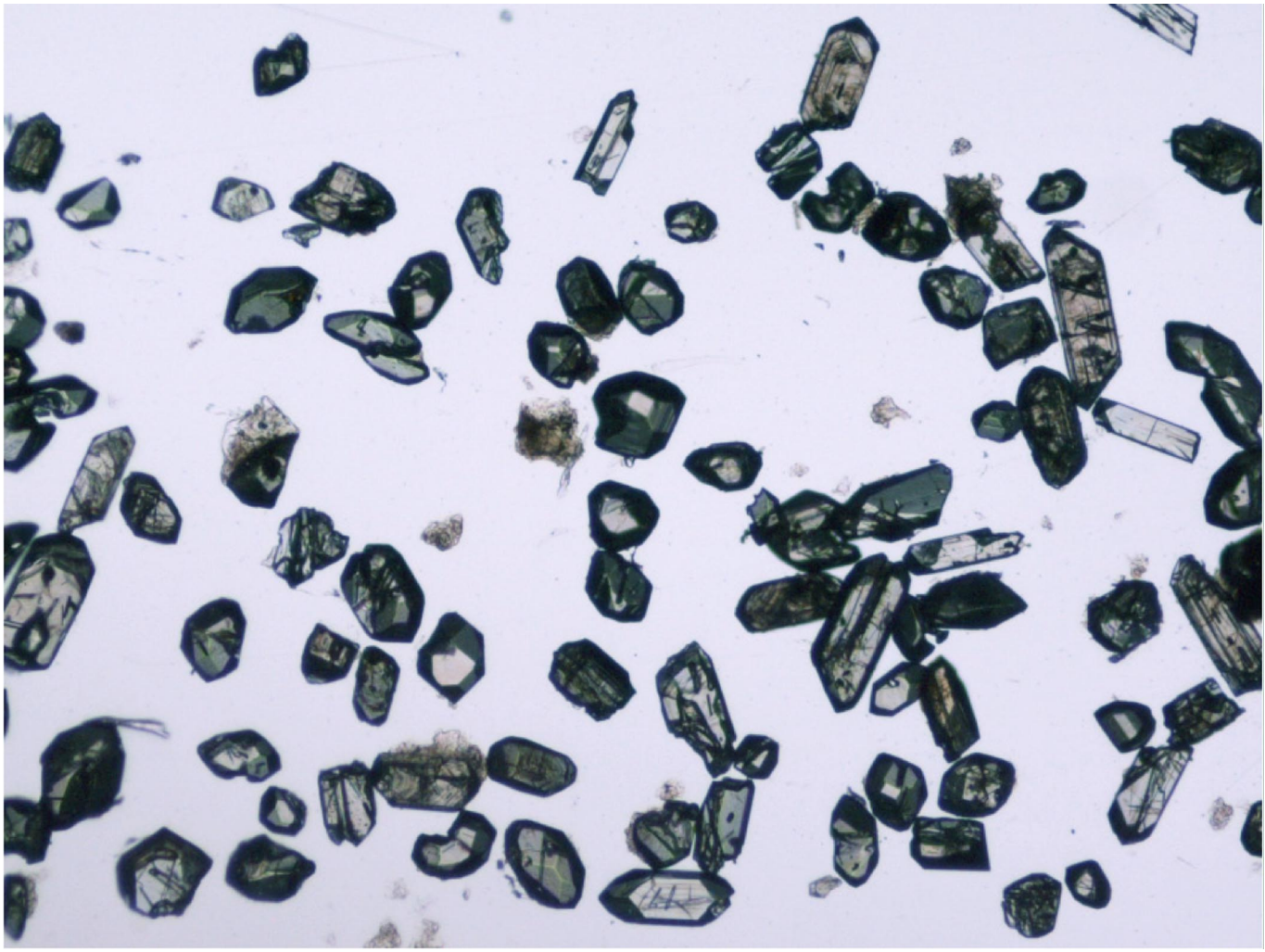

Fig. S3. Photomicrograph of zircon separates on SHRIMP mount 07–34, showing euhedral equant to prismatic crystals. Plane polarized light. Population 07–34A (sample Ind 06111202).

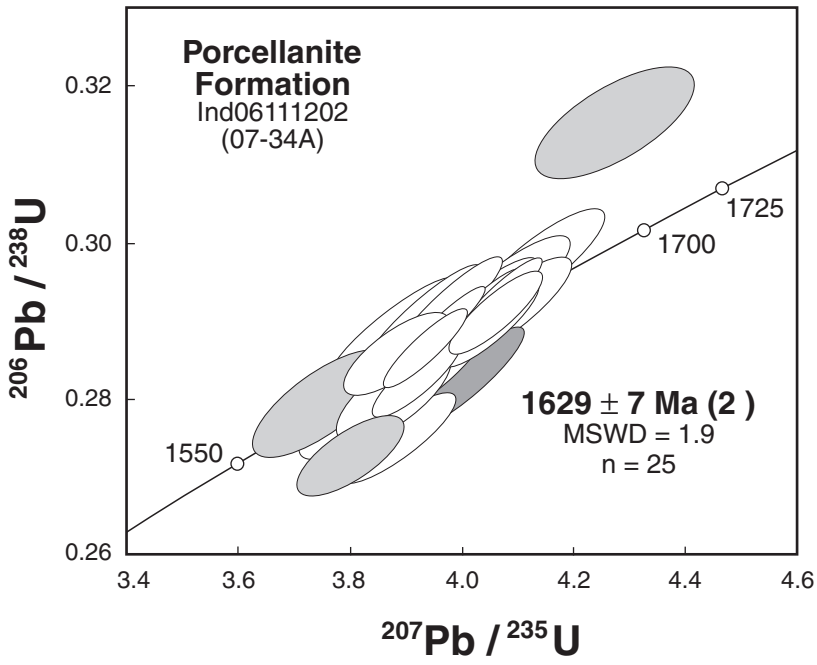

Fig. S4. Concordia plot of SHRIMP data for 07–34A (from Table S1). Light gray shading indicates analyses not used for age determination; dark gray ellipse is an older age outlier.

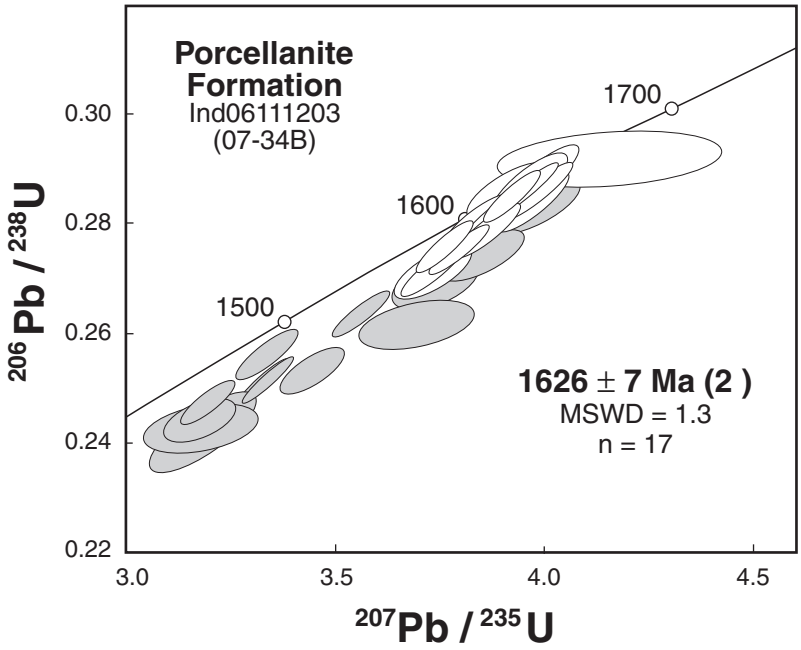

Fig. S5. Concordia plot of the most concordant SHRIMP data for 07–34B (from Table S2). Light gray shading indicates analyses not used for age determination.

Table S1. SHRIMP U–Pb data for 07–34A zircon (Sample Ind06111202) (see Fig. S4)

Analysis spot	U, ppm	Th, ppm	Th/U	f206, %	$^{207}Pb^*/^{206}Pb^*$	±	$^{206}Pb^*/^{238}U$	±	$^{207}Pb^*/^{235}U$	±	$^{208}Pb^*/^{232}Th$	±	$^{207}Pb^*/^{206}Pb^*$ Conc., %	Age, Ma	± Ma
Best data, in order of $^{207}Pb/^{206}Pb$															
0734A.1–1	40	67	1.73	0.121	0.0982	0.0014	0.2879	0.0052	3.899	0.090	0.0832	0.0018	103	1591	27
0734A.9–1	65	113	1.78	0.060	0.0985	0.0009	0.2897	0.0049	3.934	0.077	0.0818	0.0016	103	1596	18
0734A.31–1	113	137	1.25	0.114	0.0986	0.0010	0.2857	0.0035	3.883	0.061	0.0792	0.0012	101	1597	19
0734A.19–1	193	230	1.23	0.211	0.0989	0.0007	0.2912	0.0047	3.969	0.069	0.0800	0.0014	103	1603	13
0734A.3–1	93	102	1.14	0.010	0.0990	0.0007	0.2876	0.0047	3.927	0.070	0.0852	0.0016	101	1606	13
0734A.16–1	120	213	1.83	0.099	0.0993	0.0008	0.2867	0.0047	3.926	0.072	0.0830	0.0021	101	1612	15
0734A.22–1	66	102	1.59	0.036	0.0994	0.0012	0.2795	0.0048	3.830	0.080	0.0805	0.0016	99	1612	22
0734A.12–1	113	185	1.70	−0.023	0.0994	0.0008	0.2838	0.0046	3.891	0.071	0.0806	0.0014	100	1613	16
0734A.15–1	251	133	0.55	−0.004	0.0995	0.0004	0.2873	0.0045	3.943	0.063	0.0827	0.0014	101	1615	8
0734A.28–1	209	342	1.69	0.024	0.0997	0.0006	0.2864	0.0033	3.936	0.050	0.0800	0.0012	100	1618	10
0734A.8–1	120	205	1.77	0.010	0.1001	0.0007	0.2864	0.0046	3.955	0.069	0.0841	0.0015	100	1627	13
0734A.23–1	78	72	0.95	0.038	0.1003	0.0009	0.2906	0.0048	4.017	0.075	0.0846	0.0017	101	1629	16
0734A.26–1	102	141	1.42	0.371	0.1004	0.0012	0.2802	0.0035	3.878	0.067	0.0739	0.0012	98	1631	22
0734A.10–1	106	176	1.72	−0.010	0.1004	0.0006	0.2895	0.0047	4.008	0.070	0.0837	0.0015	100	1631	12
0734A.29–1	170	226	1.38	0.044	0.1006	0.0007	0.2826	0.0033	3.921	0.052	0.0796	0.0012	98	1635	12
0734A.2–1	55	76	1.44	−0.046	0.1007	0.0009	0.2871	0.0050	3.986	0.078	0.0826	0.0016	99	1637	16
0734A.21–1	136	249	1.89	−0.046	0.1007	0.0006	0.2909	0.0047	4.040	0.069	0.0839	0.0015	101	1637	11
0734A.6–1	99	135	1.41	−0.062	0.1007	0.0010	0.2936	0.0048	4.077	0.078	0.0862	0.0017	101	1637	18
0734A.18–1	335	262	0.81	0.054	0.1008	0.0005	0.2781	0.0043	3.866	0.062	0.0807	0.0014	97	1639	8
0734A.5–1	57	62	1.12	−0.126	0.1009	0.0010	0.2967	0.0051	4.130	0.081	0.0873	0.0020	102	1641	18
0734A.17–1	125	147	1.22	−0.066	0.1011	0.0007	0.2850	0.0046	3.974	0.070	0.0832	0.0015	98	1645	13
0734A.27–1	135	174	1.33	−0.040	0.1012	0.0007	0.2909	0.0035	4.058	0.057	0.0823	0.0012	100	1646	13
0734A.11–1	152	196	1.33	−0.031	0.1014	0.0006	0.2836	0.0045	3.964	0.067	0.0801	0.0014	98	1649	10
0734A.25–1	137	171	1.29	−0.015	0.1016	0.0007	0.2893	0.0036	4.053	0.057	0.0831	0.0012	99	1653	13
0734A.13–1	96	167	1.80	−0.126	0.1017	0.0009	0.2910	0.0047	4.080	0.076	0.0849	0.0015	99	1655	17
0734A.20–1	86	153	1.85	0.155	0.1017	0.0015	0.2757	0.0046	3.866	0.085	0.0797	0.0015	95	1656	27
3σ outlier (xenocryst)															
0734A.4–1	150	245	1.68	−0.058	0.1028	0.0009	0.2824	0.0045	4.001	0.072	0.0834	0.0014	96	1675	15
>5% discordant															
0734A.24–1	116	155	1.38	0.498	0.1011	0.0012	0.2726	0.0034	3.800	0.064	0.0786	0.0012	94	1645	22
>0.5% common ^{206}Pb															
0734A.14–1	139	242	1.80	0.516	0.0973	0.0013	0.2793	0.0045	3.747	0.079	0.0764	0.0017	101	1573	26
0734A.30–1	197	366	1.92	1.067	0.0982	0.0016	0.3155	0.0047	4.274	0.093	0.0870	0.0012	111	1591	30

Analyses A.1–A.23 on September 12, 2007. Pb/U calibrated against BR266 [$n = 14$; excess scatter of 1.5% (1σ) propagated to sample data]. Element abundances calibrated against U content of CZ3. Analyses A.24–A.30 on December 10, 2007 (with 07–34B; see Table 2). Listed precisions are 1σ.

*All listed Pb isotope data are corrected for common Pb on the basis of measured $^{204}Pb/^{206}Pb$ and the Stacey and Kramers model Pb composition at the sample age [Stacey JS, Kramers JD (1975) Approximation of terrestrial lead isotope evolution by a two-stage model. *Earth Planet Sci Lett* 26:207–221].

Table S2. SHRIMP U–Pb data for 07–34B zircon (Sample Ind06111203) (see Fig. S5)

Analysis spot	U, ppm	Th, ppm	Th/U	f206, %	$^{207}Pb^*/^{206}Pb^*$	±	$^{206}Pb^*/^{238}U$	±	$^{207}Pb^*/^{235}U$	±	$^{208}Pb^*/^{232}Th$	±	$^{207}Pb^*/^{206}Pb^*$ Conc., %	Age, Ma	± Ma
Best data, in order of $^{207}Pb/^{206}Pb$															
734B.10–1	624	576	0.95	0.076	0.0989	0.0005	0.2758	0.0030	3.761	0.045	0.0768	0.0010	98	1603	9
734B.23–1	168	114	0.70	0.491	0.0990	0.0011	0.2862	0.0034	3.906	0.063	0.0754	0.0015	101	1605	20
734B.31–1	223	156	0.72	0.328	0.0994	0.0008	0.2803	0.0032	3.840	0.054	0.0718	0.0011	99	1613	15
734B.30–1	456	259	0.59	0.045	0.0997	0.0004	0.2812	0.0034	3.864	0.049	0.0786	0.0010	99	1618	7
734B.25–1	397	278	0.72	0.244	0.0998	0.0006	0.2712	0.0030	3.730	0.047	0.0680	0.0009	96	1620	11
734B.24–1	175	157	0.92	0.469	0.0999	0.0011	0.2711	0.0032	3.734	0.061	0.0635	0.0011	95	1623	21
734B.3–1	125	78	0.65	0.225	0.1000	0.0008	0.2878	0.0033	3.969	0.057	0.0830	0.0017	100	1624	16
734B.8–1	465	305	0.68	0.215	0.1000	0.0005	0.2752	0.0030	3.796	0.046	0.0749	0.0010	96	1625	9
734B.15–1	159	117	0.76	0.091	0.1001	0.0007	0.2852	0.0034	3.936	0.054	0.0744	0.0011	100	1626	13
734B.11–1	192	123	0.66	0.141	0.1001	0.0008	0.2890	0.0036	3.990	0.060	0.0796	0.0015	101	1626	16
734B.5–1	251	165	0.68	0.061	0.1001	0.0005	0.2863	0.0032	3.953	0.048	0.0789	0.0010	100	1626	8
734B.33–1	156	105	0.69	0.041	0.1005	0.0007	0.2853	0.0034	3.955	0.053	0.0796	0.0012	99	1634	12
734B.26–1	441	368	0.86	0.417	0.1005	0.0007	0.2792	0.0031	3.870	0.050	0.0769	0.0011	97	1634	12
734B.27–1	96	51	0.55	0.017	0.1008	0.0011	0.2849	0.0036	3.959	0.065	0.0779	0.0018	99	1638	19
734B.34–1	200	166	0.86	0.079	0.1008	0.0006	0.2852	0.0033	3.965	0.052	0.0816	0.0011	99	1640	11
734B.7–1	215	152	0.73	0.008	0.1010	0.0005	0.2866	0.0033	3.992	0.050	0.0773	0.0010	99	1643	9
734B.28–1	139	101	0.75	−0.050	0.1015	0.0007	0.2836	0.0034	3.969	0.054	0.0786	0.0012	97	1652	12
734B.2–1	179	124	0.72	0.486	0.1031	0.0042	0.2933	0.0034	4.170	0.176	0.0875	0.0045	99	1681	75
>5% discordant															
734B.6–1	741	445	0.62	0.105	0.0963	0.0003	0.2517	0.0027	3.344	0.038	0.0693	0.0008	93	1554	6
734B.22–1	681	381	0.58	0.063	0.0961	0.0004	0.2510	0.0027	3.327	0.039	0.0693	0.0008	93	1551	8
734B.1–1	808	497	0.63	0.116	0.0954	0.0016	0.2405	0.0049	3.163	0.083	0.0670	0.0017	90	1536	31
>0.5% common ^{206}Pb															
734B.4–1	751	567	0.78	0.632	0.0936	0.0006	0.2468	0.0027	3.186	0.040	0.0663	0.0008	95	1500	13
734B.12–1	816	907	1.15	0.665	0.0946	0.0007	0.2560	0.0031	3.337	0.047	0.0705	0.0009	97	1519	14
734B.32–1	105	89	0.88	0.869	0.1013	0.0017	0.2837	0.0035	3.960	0.082	0.0662	0.0016	98	1647	30
734B.14–1	1238	954	0.80	1.012	0.0810	0.0008	0.1881	0.0021	2.100	0.031	0.0514	0.0007	91	1220	20
734B.13–1	553	346	0.65	1.061	0.0988	0.0010	0.2531	0.0028	3.447	0.051	0.0648	0.0011	91	1601	18
734B.29–1	235	172	0.75	1.325	0.1017	0.0014	0.2744	0.0031	3.846	0.070	0.0769	0.0015	94	1655	26
734B.18–1	710	678	0.99	1.860	0.0943	0.0014	0.2432	0.0027	3.163	0.058	0.0653	0.0010	93	1515	28
734B.21–1	418	424	1.05	1.921	0.1008	0.0015	0.2692	0.0030	3.742	0.071	0.0744	0.0012	94	1639	28
734B.35–2r	499	508	1.05	3.210	0.0955	0.0027	0.1826	0.0021	2.404	0.073	0.0341	0.0011	70	1537	52
734B.16–1	601	398	0.68	3.217	0.1025	0.0022	0.2614	0.0029	3.695	0.091	0.0728	0.0019	90	1671	40
734B.17–1	408	308	0.78	3.298	0.0947	0.0024	0.2416	0.0029	3.156	0.089	0.0613	0.0017	92	1523	48
734B.35–1c	1784	975	0.56	4.004	0.0755	0.0028	0.1231	0.0014	1.281	0.049	0.0300	0.0012	69	1081	74
734B.19–1	771	688	0.92	4.113	0.0903	0.0027	0.2097	0.0024	2.612	0.085	0.0476	0.0013	86	1432	58
734B.20–1	413	319	0.80	9.691	0.1021	0.0133	0.2138	0.0038	3.011	0.396	0.0576	0.0075	75	1663	241
4σ outlier															
734B.9–1	608	380	0.65	0.123	0.0980	0.0005	0.2635	0.0029	3.563	0.044	0.0727	0.0010	95	1587	10

Analyzed on December 10, 2007. Pb/U calibrated against BR266 [n = 11; excess scatter of 1.06% (σ) propagated to sample data]. Element abundances calibrated against U content of CZ3. Listed precisions are 1σ.

*All listed Pb isotope data are corrected for common Pb on the basis of measured $^{204}Pb/^{206}Pb$ and the Stacey and Kramers model Pb composition at the sample age [Stacey JS, Kramers JD (1975) Approximation of terrestrial lead isotope evolution by a two-stage model. *Earth Planet Sci Lett* 26:207–221].

Table S3. ICPM MS data from phosphorites (see Fig. 5)

Sample ID	$^{206}Pb/^{204}Pb$	$^{207}Pb/^{204}Pb$	$^{208}Pb/^{204}Pb$
06110805 whole rock 1	38.586	17.812	43.315
06110805 whole rock 2	38.570	17.811	42.953
06110805 leachate	40.206	17.968	43.817
06110805 residue	31.493	17.109	40.575
06110701 whole rock	29.981	16.922	40.102